ISSN (Print) 1226-1750
ISSN (Online) 2233-6656
Journal of Magnetics 27(2), 223-231 (2022) https://doi.org/10.4283/JMAG.2022.27.2.223

Hall Current and Viscous Dissipation Impact on MHD Mixed Convection Flow towards a Porous Exponentially Surface with its Engineering Applications

Aaqib Majeed[1], Ahmad Zeeshan[2], Aqila Shaheen[3], Mohammed Sh. Alhodaly[4], and Farzan Majeed Noori[5]*

[1]*Department of Mathematics, The University of Faisalabad, Sargodha Road, University Town Faisalabad, 38000, Pakistan*
[2]*Department of Mathematics and Statistics, FBAS, International Islamic University Islamabad, H-10, Islamabad, 44000, Pakistan*
[3]*Department of Mathematics, Minhaj University Lahore, Lahore 54770, Pakistan*
[4]*Nonlinear Analysis and Applied Mathematics (NAAM) Research Group, Department of Mathematics, Faculty of Science, King Abdulaziz University, Jeddah 21589, Saudi Arabia*
[5]*Department of Informatics, Faculty of Mathematics and Natural Sciences, University of Oslo, 4959, Oslo, Norway*

(Received 18 May 2021, Received in final form 21 May 2022, Accepted 8 June 2022)

Power generators, Hall accelerators, and flight MHD all require high levels of Hall current. The influence of Hall current and viscous dissipation on time-independent hydro-magnetic mixed convective radiative flow across a porous heated surface has thus been investigated using numerical computing and mathematical modeling in the current study. The fluid is electrically conducted and varies exponentially. It is assumed that the wall temperature and elongation rate will vary with specific exponential shapes. A solid uniform magnetic field B_0 is employed normally to the surface. The mathematical model of PDEs for incompressible flow is transformed into ODE by applying a numerical technique based on a finite-difference structure which includes a three-stage Lobatto IIIa scheme with the help of MATLAB. The obtained solution depends on the convergence constraints involving the radiation parameter R, magnetic parameter M, porosity parameter Ω, Hall parameter m, buoyancy parameter ε, temperature distribution parameter a, Eckert number E_c, Prandtl number P_r, and convective term bh. Graphs of the velocity and temperature profiles are explained via pertinent parameters. Skin friction factor, and Nusselt number are also evaluated and presented graphically and in tabular form. Results clarify that temperature profile reduces by increasing values of temperature distribution parameter whereas opposite behavior is noted for positive values of the buoyancy parameter.

Keywords : hall current, porous medium, mixed convection, MHD, thermal radiation, viscous dissipation, numerically

1. Introduction

Flows over an exponentially stretched surface attract the various researchers due to their wider range of applications in various technological, industrial, and engineering developments such as crystal growth, metallic sheet cooling, aerodynamics extrusion of plastic, fluid film condensation, sheets, polymer industries, structural making of chemical processing things, and anaerobic extrusion of plastic sheets. As several metal cycles require continuous cooling of strips, the problem of MHD has recently become more visible in the industry. When in the presence of a magnetized field, the cooling rate can be adjusted by immersing them in an electrically conductive fluid. Sakiadis [1, 2] was the first to draw the attention to the need for a stretchable surface under certain situations, the valuable efforts of Sakiadis were more deeply studied by several researchers, including different flow patterns in which examination of mass transfer toward an expanding surface along with convective boundary condition occurs, these are the conditions for heating up convicting fluids by applying heat in limited amount through boundaries of the surfaces which causes the rate of interchange of heat through the boundary which is in direct relation to (T_o-T_∞). Due to these conditions, the exploration of heat transfer has gained great importance in the fields of mechanics. Merkin [3] analyzed the consequence of natural convection boundary layer flow normal to sheet with Newtonian heating. Pattnaik *et al*. [4] examined the nanofluid flow over a vertical surface adjacent to a porous medium by considering Eringen's micropolar model.

Shahid *et al*. [5] described the physical features of

*Corresponding author: Tel: +47 91255115
Fax: +47 91255115, e-mail: farzanmn@ifi.uio.no

magneto-hydrodynamics (MHD) Carreau nanofluid bi-convection flow past an upper paraboloid porous surface. Hayat *et al*. [6] deliberated the heat and mass transfer analysis by considering Eyring-Powell fluid past an inclined exponential expanding surface. The impact of convective boundary conditions and thermal Biot number on different kinds of fluids past an exponentially stretching sheet is investigated by various researchers [7-10]. Wong *et al*. [11] inspected the viscous dissipation impact on time-independent fluid flow near an exponentially stretching/shrinking surface.

The effort exerted by a fluid on adjacent layers due to the action of shear forces is converted into heat in a viscous dissipation loop. Gehbart [12] explored the implication of viscous dissipation by assuming natural convection. Das [13] investigated the consequences of magnetized flow of mass and heat transport analysis over a semi-infinite plate. Megahed [14] examined the consequences of heat transfer utilizing viscous dissipation and slip velocity factors on Casson liquid flow over a time-dependent surface.

An orthogonal induced current to electric and magnetic fields is termed a Hall current. If there exists a magnetic field, this is critical since the normal conductivity to the magnetized field weakens owing to the free production of electrons and particles along the lines of an attractive field until it crashes into ionized gas with a low thickness or a solid magnetic field. Gupta [15] investigated the impact of Hall parameter on magneto-hydrodynamic flow over an absorbent sheet. Hayat *et al*. [16] considered the Hall impact on second-grade rotating liquid flow and heat transfer past a porous sheet. Aziz *et al*. [17] discovered an expression which deliberates the impacts of internal heating on MHD flow due to expanding surface with Hall current. Aziz and Nabil [18] deliberated the Hall current impact on magnetic mixed convective flow over an exponentially varying surface. Recently Pal [19] premeditated the impact of radiation and Hall parameter on time-dependent viscous flow towards a permeable space. Some of the recent articles related to our study can be seen in Ref. [20-24].

The motivation of the current exploration is to bring out the influence of the Hall parameter on magnetized mixed convective incompressible boundary layer flow towards a porous surface varying exponentially under the influence of radiation and viscous dissipation. The present result shows a remarkable application of glass fiber formation, hot moving, paper creation, wire drawing of plastic movies, metals, metal turning, and polymer expulsion are all examples of heat transfers in a two-dimensional boundary layer phenomenon. The obtained fallouts portray the effect of numerous dimensionless flowing parameters on temperature and velocity profiles with skin friction and Nusselt number graphically. Our numerical fallouts are compared with [18] and found an excellent agreement as exposed in Table 1.

2. Mathematical Formulation

Here we investigate an incompressible, unsteady, electrically conducting mixed convection flow with heat transport analysis through a semi-infinite porous vertical wall (see Fig. 1), a stretched sheet having speed of U_w

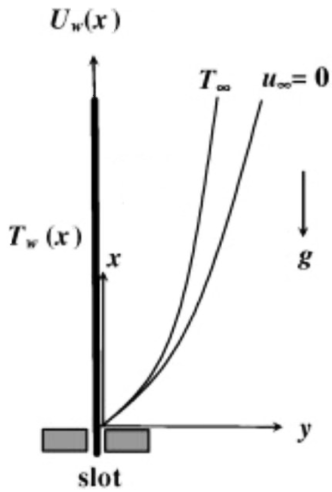

Fig. 1. Physical sketch of the problem.

Table 1. Calculation of $-\theta'(0)$ for some values of temperature distribution parameter a and Prandtl number P_r by taking M, m, ε, Ω and E_c equal to zero and $R \to \infty$.

For	a=1.0		a= -0.5,		a=0.0,	
P_r	Ref. [18]	Present	Ref. [18]	Present	Ref. [18]	Present
0.5	0.174455	0.173334	0.330824	0.320319	0.594112	0.561212
1	0.299795	0.291147	0.549589	0.521008	0.955325	0.871567
3	0.635700	0.596482	1.123344	1.008882	1.869397	1.574743
5	0.874551	0.870594	1.524815	1.320378	2.500382	2.000084
10	1.309138	1.545349	2.256776	1.841683	2.673949	2.679555

and a temperature of T_w, which is moving through a stationary sludge fluid flow with a constant temperature T_∞ and a convective state. The rectangular coordinate axes are the x and y-axis characterizes towards and perpendicular to the surface. It's also believed that the z-axis runs parallel to the sheet's leading edge.

The fluid is emitting/absorbing radiation and heat flux is designated by considering the Roseland approximation in the energy equation. A strong magnetic field B_0 in the transverse direction is also applied along the y-axis. Meanwhile, the magnetized Reynolds number is supposed to be very less i.e. ($R_{em} << 1$), hence the induced magnetic field is considered negligible. It is worth notable that Hall current develop a rising force in the z-direction when the there is a strong magnetic field, a cross-flow pattern is shown there in the z-direction and hereafter the flow converts into 3-D, assuming that no deviation of flow occurs along the z-direction as the sheet is infinite in that direction. The following could be true if the Hall definition is engaged in generalized Ohm's law [18]:

$$J + \frac{w_e \cdot \tau_e}{B_0}(J \times B) = \sigma\left(E + V \times B + \frac{1}{en_e}\nabla P_e\right). \tag{1}$$

Here V specify the velocity vector, $B = (0, B_0, 0)$ represent the magnetic induction vector, $J = (J_x, J_y, J_z)$ signify the current density vector, τ_e explain the electron collision time, w_e identify the cyclotron frequency of electron, and σ specify the electrical conductivity. It is also noted that $w_i \cdot \tau_i < 1$, where w_i and τ_i represent the cyclotron frequency and collision time for ions, respectively, and the short circuit case is assumed where $E = 0$ (applied electric field), electron pressure gradient may be ignored for partially ionized gas. Supposing the plate is a non-conductor of electricity, keeping the above assumption in view the generalized form of Ohm's law gives ($J_y = 0$) in all the places in the flow field. By taking x and z components from the above equation (1) and resolving for the components J_x and J_z we get:

$$J_x = \frac{\sigma B_0}{(1 + m^2)}(mu - w), \tag{2}$$

$$J_z = \frac{\sigma B_0}{(1 + m^2)}(u - mw). \tag{3}$$

Where u, v, w represents the apparatuses of velocity vector V in (x, y, z) directions and $m = w_e \cdot \tau_e$ indicates the Hall parameter.

The equations of motion govern the flow are given below [18]:

$$\frac{\partial u}{\partial x} + \frac{\partial v}{\partial x} = 0, \tag{4}$$

$$u\frac{\partial u}{\partial x} + v\frac{\partial u}{\partial y} = v\frac{\partial^2 u}{\partial y^2} + g\beta(T - T_\infty) - \frac{\sigma B_0^2}{\rho(1 + m^2)}(u + mw) - \frac{v}{k}u, \tag{5}$$

$$u\frac{\partial w}{\partial x} + v\frac{\partial w}{\partial y} = v\frac{\partial^2 w}{\partial y^2} + \frac{\sigma B_0^2}{\rho(1 + m^2)}(mu - w), \tag{6}$$

$$u\frac{\partial T}{\partial x} + v\frac{\partial T}{\partial y} = \alpha\frac{\partial^2 T}{\partial y^2} - \frac{1}{\rho_{cp}}\frac{\partial_{q_r}}{\partial y} + \frac{\mu}{\rho_{cp}}\left[\left(\frac{\partial u}{\partial y}\right)^2 + \left(\frac{\partial w}{\partial y}\right)^2\right]. \tag{7}$$

Here $\alpha = \frac{k}{\rho_{cp}}$ signify thermal diffusivity where k signify thermal conductivity of the fluid and c_p exemplify heat capacity, $v = \frac{\mu}{\rho}$ represents coefficient of kinematic viscosity and T represent fluid temperature, ρ is density. q_r illustrate the radiative heat flux, after approximation, it may attain the form:

$$q_r = -\frac{4\sigma 1}{4k_1}\frac{\partial T^4}{\partial y}, \tag{8}$$

where $\sigma 1$ indicates the Boltzman constant and k_1 shows the mean absorption coefficient. Expanding T^4 by Taylor's series up to T_∞ ignoring high order terms we acquire

$$T_\infty = 4T_\infty^3 T - 3T_\infty^3, \tag{9}$$

In the light of the above expressions (8, 9), equation (7) can be written as [25]:

$$u\frac{\partial T}{\partial x} + v\frac{\partial T}{\partial y} = \alpha\frac{\partial^2 T}{\partial y^2} + \frac{16\sigma 1 T_\infty^3}{3k_1\rho_{cp}}\frac{\partial^2 T}{\partial y^2} + \frac{\mu}{\rho_{cp}}\left[\left(\frac{\partial u}{\partial y}\right)^2 + \left(\frac{\partial w}{\partial y}\right)^2\right]. \tag{10}$$

2.1. Boundary conditions

The transformed boundary relations are

$$u = U_w,\ v = 0,\ w = 0,\ k\frac{\partial T}{\partial y} = -h(T_w - T),\ \text{at } y = 0, \tag{11}$$

$$u \to 0,\ w \to 0,\ T \to T_\infty, \quad \text{at } y \to \infty. \tag{12}$$

It is considered that the stretching sheet has an exponential velocity distribution as defined below in equation (13).

$$U_w = U_0 \exp\left(\frac{x}{L}\right), \tag{13}$$

where L indicates the reference length, U_0 is the constant value. Notably, the exponential velocity defined in the above equation is valid when $x << L$.

Wall temperature of the sheet is considered as:

$$T_w = T_\infty + T_0 \exp\left(\frac{ax}{2L}\right). \tag{14}$$

Here a and T_0 are temperature distribution parameters, and T_∞ is the ambient temperature.

Velocity components u and v are instigated from the following:

$$u = \frac{\partial \psi}{\partial y} \text{ and } v = -\frac{\partial \psi}{\partial x}, \tag{15}$$

where $\psi(x, y) = \sqrt{2\nu L U_0} \exp\left(\frac{x}{L}\right) f(\eta)$,

here $\eta = y\sqrt{\frac{U_0}{2\nu L}} \exp\left(\frac{x}{2L}\right)$, (16)

Similarly $w = U_0 \exp\left(\frac{x}{L}\right) h(\eta)$,

and $T = T_\infty + (T_w - T_\infty)\theta(\eta)$. (17)

Using the above similarity variables defined in the above equations, new velocity components can be expressed as:

$$u = U_0 \exp\left(\frac{x}{L}\right) f'(\eta),\ v = -\sqrt{\frac{\nu U_0}{2L}} \exp\left(\frac{x}{2L}\right)(f + \eta f'). \tag{18}$$

Using all the above terms defined in (15-18), we get the ordinary differential equations as follows:

$$f''' + ff'' - 2f'^2 + 2\varepsilon\theta - \Omega f' - \frac{2M(f' + mh)}{(1 + m^2)} = 0, \tag{19}$$

$$h'' + h'f - 2hf' + \frac{2M(f' - h)}{(1 + m^2)} = 0, \tag{20}$$

$$\left(1 + \frac{4}{3R}\right)\theta'' + P_r.E_c(f''^2 + h'^2) + P_r(f\theta' - af'\theta) = 0. \tag{21}$$

The boundary conditions defined in equations (11, 12) are then transformed as:

$$f'(0) = 1, f(0) = 0, h(0) = 0, \theta'(0) = -bh(1 - \theta(0)), \tag{22}$$

$$f'(\infty) \to 0, h(\infty) \to 0, \theta(\infty) \to 0, \tag{23}$$

The pertinent dimensionless parameters that appear in the above equations are

$$\text{Here } \lambda = \frac{Gr_x}{Re_x^2},\ Gr_x = \frac{g\beta(T_w - T_\infty)L^3}{\nu^2},\ Re_x = \frac{U_w L}{\nu},$$

$$\Omega = \frac{2\nu L}{U_0 \exp\left(\frac{x}{L}\right) k},\ M = \frac{\sigma 1 B_0^2 L}{\rho U_w},\ R = \frac{kk_1}{4\sigma T_\infty^3},\ P_r = \frac{\nu}{\alpha},$$

$$\alpha = \frac{k}{\rho cp},\ E_c = \frac{U_w^2}{cp(T_w - T_\infty)},\ bh = \frac{h}{k}\sqrt{\frac{2\nu L}{U_w}}. \tag{24}$$

Quantities of the main interest which are having some practical applications are friction factor and heat transfer rate defined in equations (25) are:

$$C_{fx} = \frac{2\tau_{wx}}{\rho U_w^2} = \frac{2\mu\left(\frac{\partial u}{\partial y}\right)_{y=0}}{\rho U_w^2} = \frac{\sqrt{2}.f''(0)}{\sqrt{Re_x}},$$

$$C_{fz} = \frac{2\tau_{wz}}{\rho U_w^2} = \frac{2\mu\left(\frac{\partial w}{\partial y}\right)_{y=0}}{\rho U_w^2} = \frac{\sqrt{2}.h'(0)}{\sqrt{Re_x}},$$

$$N_{nx} = \frac{-L}{(T_w - T_\infty)}\left(\frac{\partial T}{\partial y}\right)_{y=0} = -\frac{1}{\sqrt{2}}\sqrt{Re_x}.\theta'(0). \tag{25}$$

3. Results and Discussion

In this portion, graphical results are drawn against physical parameters like temperature distribution parameter a, Eckert number E_c, buoyancy parameter ε, magnetic parameter M, hall parameter m, radiation parameter R, porosity parameter Ω, and convective parameter bh. The influence of temperature distribution term a on velocity and temperature fields is observed in Figs. 2-4, from a physical point of view, Fig. 4 demonstrates that the temperature profile is decreased by the increasing values of temperature distribution parameter a. The reduced temperature directly impacts the buoyancy forces, which decelerate the velocity profiles that can be seen in Figs. 2 and 3.

Fig. 5 elaborates the temperature profile for several values of Eckert number E_c. The figure demonstrates that temperature enhances with growing the value of E_c. It's because friction between the fluid components causes

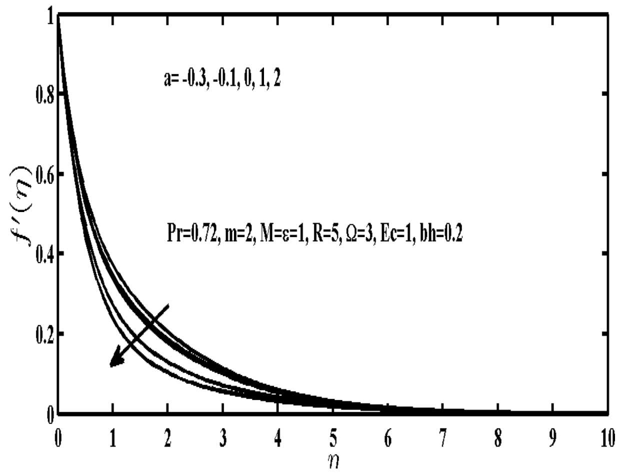

Fig. 2. Inspiration of temperature distribution parameter a on $f'(\eta)$.

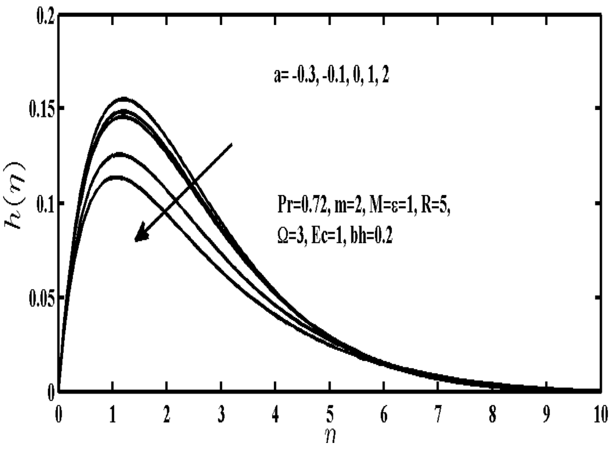

Fig. 3. Inspiration of temperature distribution parameter a on $h(\eta)$.

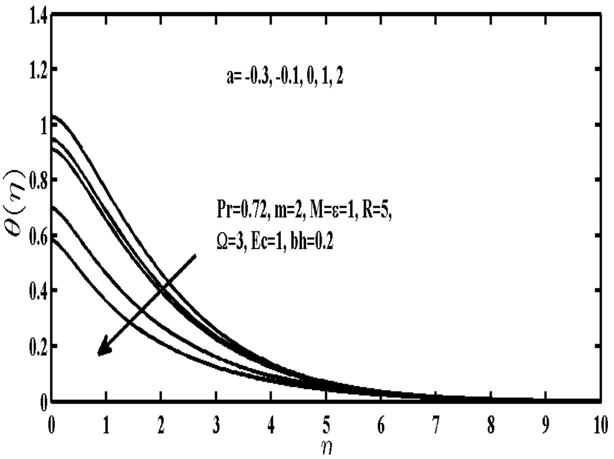

Fig. 4. Inspiration of temperature distribution parameter a on $\theta(\eta)$.

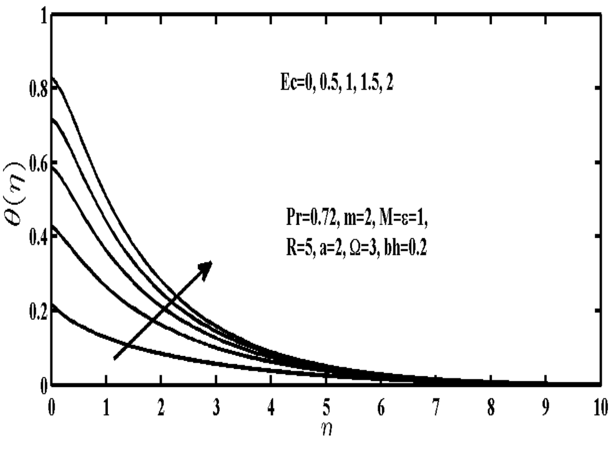

Fig. 5. Inspiration of Eckert number E_c on $\theta(\eta)$.

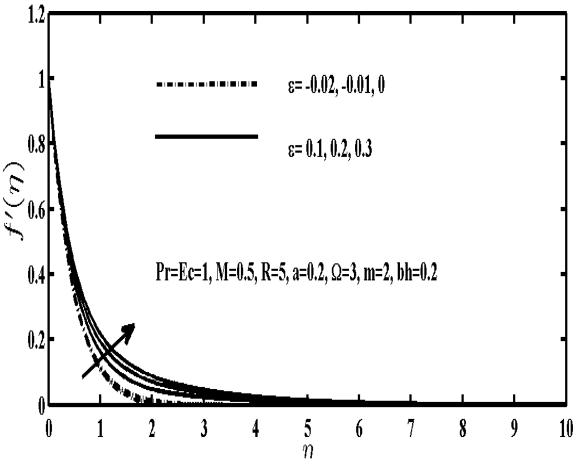

Fig. 6. Inspiration of buoyancy parameter ε on $f'(\eta)$.

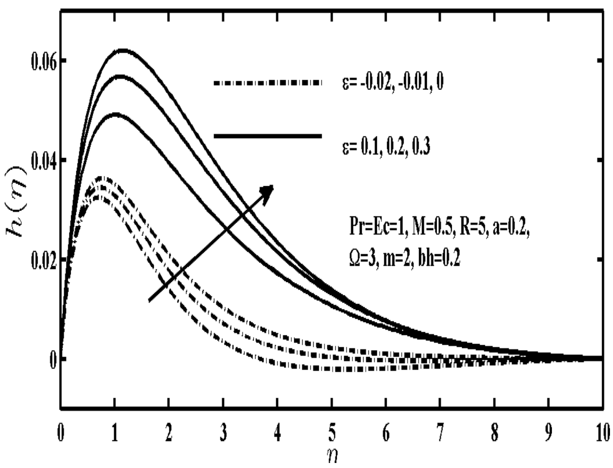

Fig. 7. Inspiration of buoyancy parameter ε on $h(\eta)$.

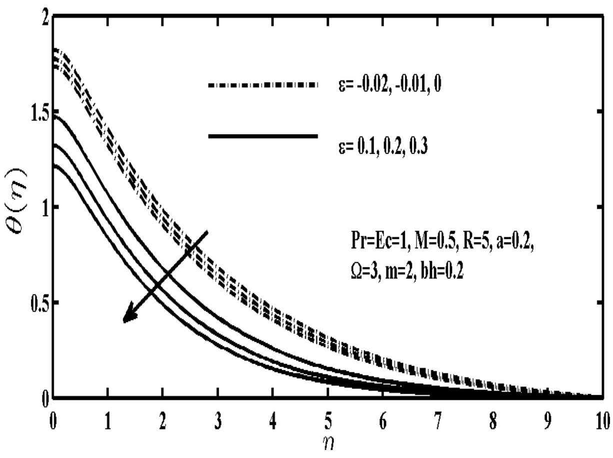

Fig. 8. Inspiration of buoyancy parameter ε on $\theta(\eta)$.

viscous dissipation to produce more heat for various buoyancy parameter ε values, the velocity and temperature profiles are presented in Figs. 5-7. In Fig. 6 it is seen that $f'(\eta)$ enhances assisting the flow of the buoyancy parameter ε while it shows decrement in the physics for opposing flow of ε. It is because of the fact that positive buoyancy persuades an advantageous pressure gradient that boosts up the boundary layer flow, whereas the negative value of ε yields an opposing pressure gradient that decelerates the fluid movement. Also, it may be observed in Fig. 7 that the impact of ε is the same in the case of transverse velocity field $h(\eta)$. Similarly, the positive or negative values of ε accelerate (decelerate) the flow near the momentum boundary layer, which in turn makes thinner (thicker) thermal boundary layer so that temperature field may show a decrement as mentioned in Fig. 8.

Figs. 9-11 indicates the physical view of the relationship between magnetic parameter M with velocity and temperature fields. It is shown in Figs. 9 and 11, the velocity field reduces while the fluid temperature increases among the boundary layer for higher values of magnetic parameter M. The reason for this is that the drag-like force develops by the transverse magnetic field called the Lorentz force, which tends to oppose the fluid movement alongside the surface which interns enhance the temperature. It is also apparent that by rising the numeric values of magnetic parameter a cross-flow in the transverse direction is

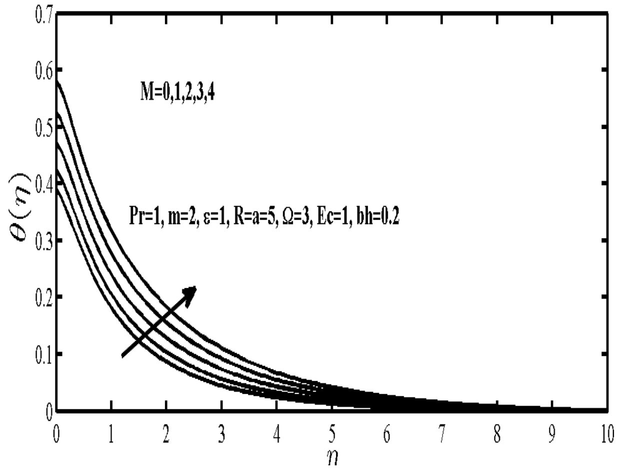

Fig. 11. Inspiration of magnetic parameter M on $\theta(\eta)$.

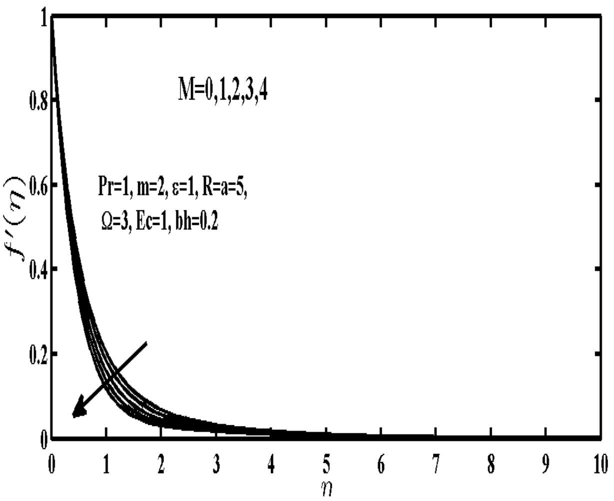

Fig. 9. Inspiration of magnetic parameter M on $f'(\eta)$.

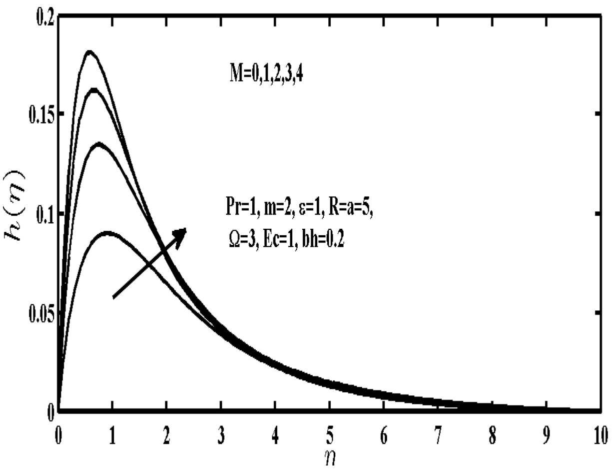

Fig. 10. Inspiration of magnetic parameter M on $h(\eta)$.

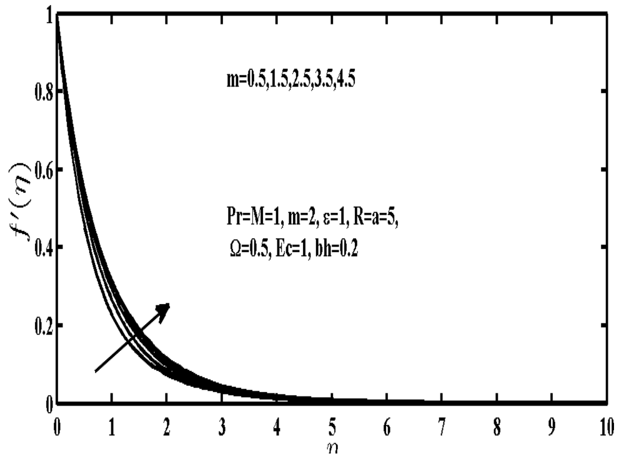

Fig. 12. Inspiration of hall parameter m on $f'(\eta)$.

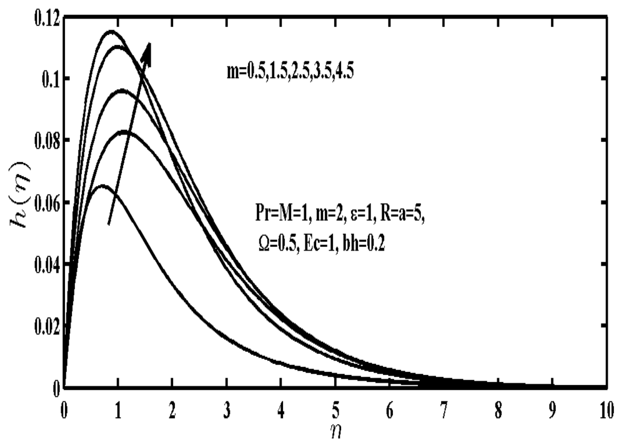

Fig. 13. Inspiration of hall parameter m on $h(\eta)$.

significantly persuaded because of Hall impact. Therefore, an increment in the transverse velocity is shown in Fig. 10.

Figs. 12-14 demonstrates physically, the outcome of m on velocity $f'(\eta)$ and temperature $\theta(\eta)$ profiles. The figure shows an increment in the velocity profile $f'(\eta)$ while the temperature field $\theta(\eta)$ in Fig. 14 shows a decrement with the variation of m. This is because the term $\frac{\sigma}{1+m^2}$ reduces while increasing the value of m which lessens the magnetic damping force on velocity field $f'(\eta)$. It is also shown from the figures that $f'(\eta)$ and $\theta(\eta)$ tends their classical hydrodynamic values for larger value of m without bounds since for enormous values of m the magnetic force terms approach zero. Fig. 13 displays that the transverse field first rises gradually and then decreases to almost zero when m is very large. In fact, in the term $\frac{\sigma}{1+m^2}$ the larger value of m is very insignificant, hence the magnetic force's resistive impact.

Figs. 15-17 establishes the radiation R impact on velocity and temperature fields. It is seen from Fig. 17, that R decreases implies $\theta(\eta)$ increased. This is because the reduction in the values of R decreases the Rosseland

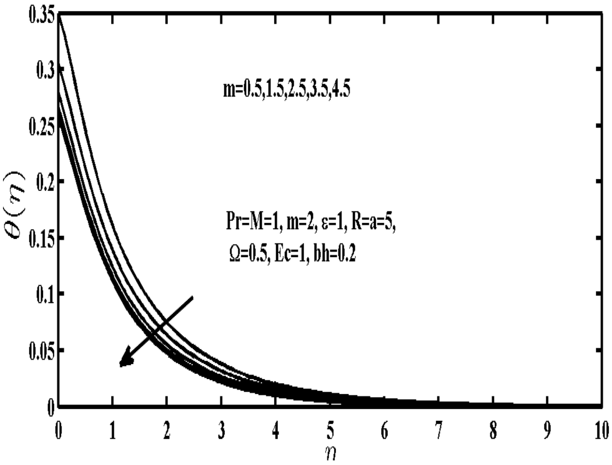

Fig. 14. Inspiration of hall parameter m on $\theta(\eta)$.

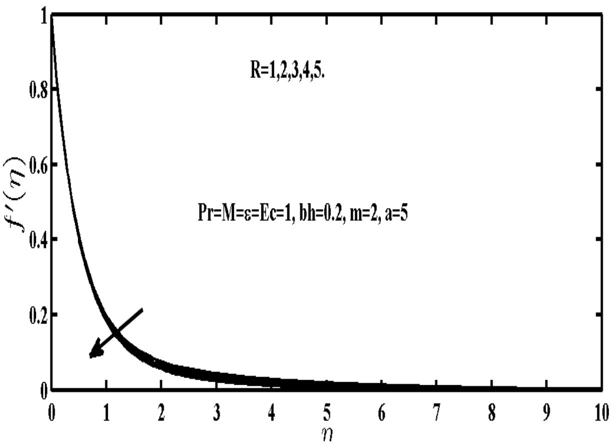

Fig. 15. Variation of radiation parameter R on $f'(\eta)$.

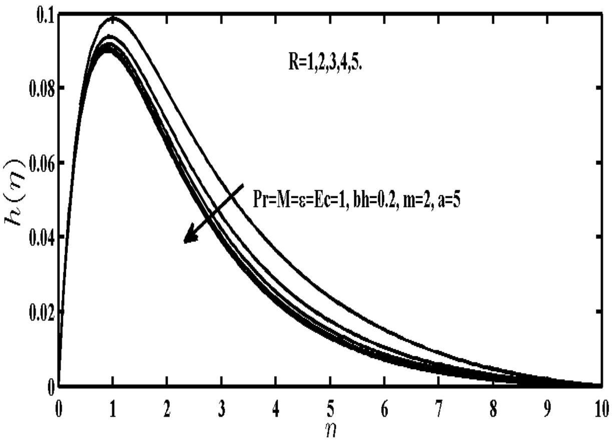

Fig. 16. Variation of radiation parameter R on $h(\eta)$.

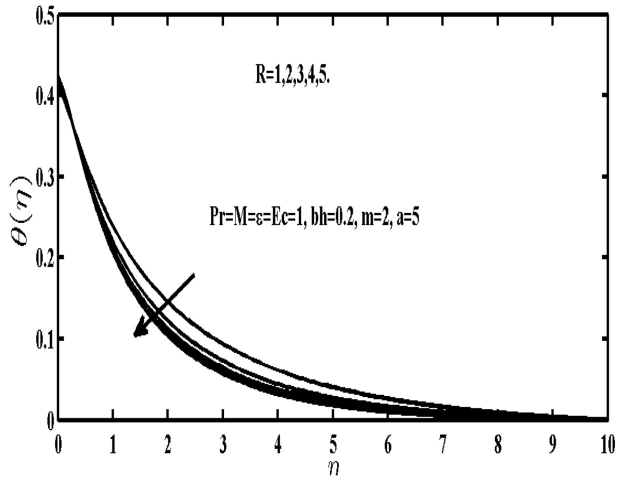

Fig. 17. Variation of radiation parameter R on $\theta(\eta)$.

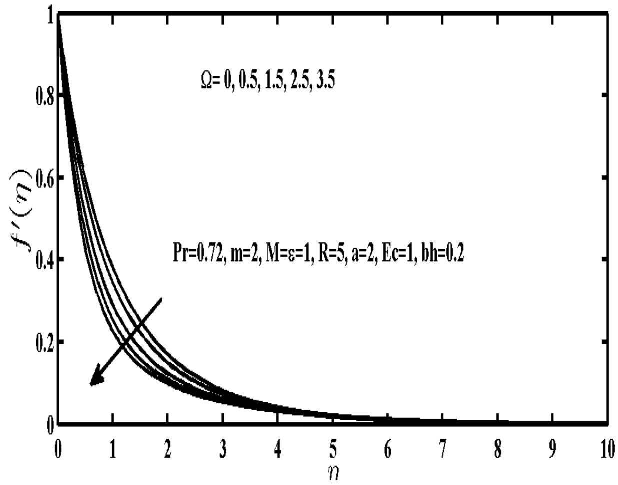

Fig. 18. Variation of porosity parameter Ω on $f'(\eta)$.

radiation absorptivity, As the Rosseland radiation absorptivity decreases, the radiative heat flux increases, increasing the radiative heat transfer rate to the fluid and thereby increasing the temperature of the fluid. The enhancement occurs in the temperature profile has direct contact with the buoyancy force which, persuades more flow in the boundary layer producing enhancement in $f'(\eta)$ and $h(\eta)$ that can be seen in Figs. 15 and 16.

Fig. 18 reveals the impact porosity parameter Ω on the velocity field $f'(\eta)$. One may observe that the velocity field reduces while increasing the value of Ω. As the whole in porous sheets become broader when the term Ω increases, a drag-like force is experienced by the fluid that may oppose the flow direction and cause reduce the fluid velocity. Fig. 19 physically describes the relationship between thermal Biot number *bh*, on temperature field $\theta(\eta)$, it can be shown that by increasing the value of bh, both boundary layer thickness and temperature are increased. The variation in the friction factor $f''(0)$ and rate of heat transfer $-\theta'(0)$ for $M = 1, 2$ and $m = 0.3, 1.5,$ 3 are physically described in Figs. 20 and 21. These figures demonstrate that $f''(0)$ and $-\theta'(0)$ decrease for several values of *m*.

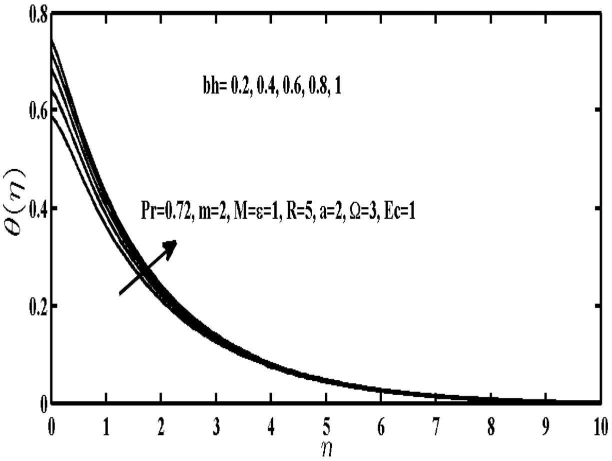

Fig. 19. Variation of convective term *bh* on $\theta(\eta)$.

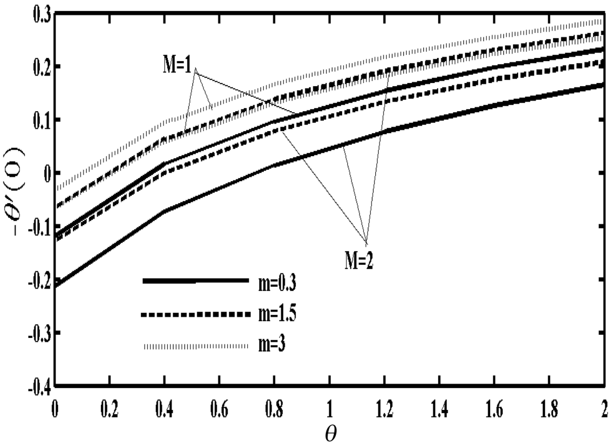

Fig. 20. Variation of Nusselt number $-\theta'(0)$ vs M.

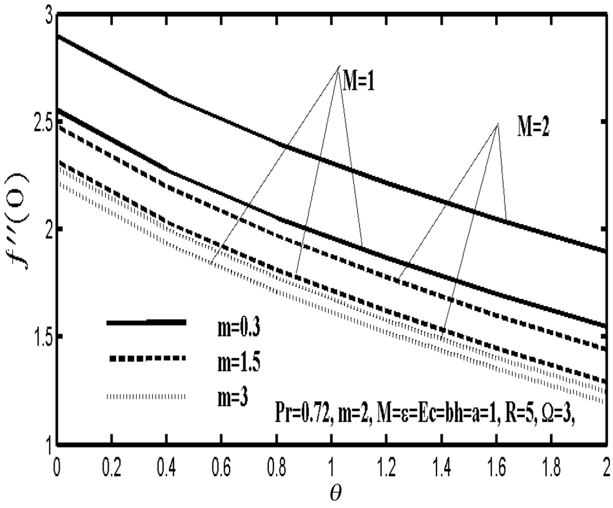

Fig. 21. Variation of skin friction $f''(0)$ vs M.

4. Concluding Remarks

In this article, we have mainly focused on the magneto-hydrodynamic (MHD) mixed convective boundary layer flow and heat transport analysis past a vertically stretchable surface under the stimulus of Hall current. The role of convergence constraints on velocity and temperature field are examined pictorially. Furthermore, the new observations against the pertinent parameters for the present study are elaborated as follows:

- Temperature profile shows decrement by increasing values of temperature distribution parameter (*a*).
- Velocity profile boost up for the positive values of the buoyancy parameter (ε) while it reduces for negative values of ε.
- Velocity field increases for Hall parameter (m) while temperature field decreases.
- Temperature profile reduces for higher values of *R*.
- Impact of a magnetic parameter (*M*) reduces the velocity profile.
- Influence of porosity parameter slowdown the velocity profile.
- Enhancement is noted in the temperature for the Biot number.

Nomenclature

R : The radiation parameter
k : Thermal conductivity

a	: The parameter of temperature distribution
c_p	: Heat capacity
P_r	: Prandtl number
v	: Coefficient of kinematic viscosity
E_c	: Eckert number
T	: Fluid temperature
Ω	: porosity parameter
ρ	: Fluid density
bh	: Thermal Biot number
q_r	: Radiative heat flux
B_0	: Uniform magnetic field
$\sigma 1$	: Boltzman constant
U_w	: Velocity of the fluid
k	: Mean absorption coefficient
T_w	: Temperature of the fluid
L	: Reference length
T_∞	: Constant temperature
ε	: Buoyancy parameter
V	: Velocity vector
Ω	: Porosity parameter
B	: Magnetic induction vector
M	: Magnetic field parameter
J	: Current density vector
m	: Hall parameter
w_e	: cyclotron frequency of electron
Gr_x	: Local Grashop number
τ_e	: Electron collision time
Re_x	: Reynolds number
σ	: Electrical conductivity
P_r	: Prandtl number
E	: Electric field
C_{fx}	: Skin-friction
α	: Thermal diffusivity
N_{ux}	: Local Nusselt number

References

[1] B. C. Sakiadis, AICHE J. **7**, 26 (1961).
[2] B. C. Sakiadis, AICHE J. **7**, 221 (1961).
[3] J. H. Merkin, Int. J. Heat Fluid Fl. **15**, 392 (1994).
[4] P. K. Pattnaik, M. M. Bhatti, S. R. Mishra, M. A. Abbas, and O. A. Bég, J. Math. **2020**, 1 (2022).
[5] A. Shahid, M. M. Bhatti, R. Ellahi, and K. S. Mekheimer, Sustain. Energy Technol. Assess **52**, 102029 (2022).
[6] T. Hayat, Y. Saeed, A. Alsaedi, and S. Asad, Plos One **10**, e0133831 (2015).
[7] M. Rahman, A. V. Rosca, and I. Pop, Int. J. Numer. Method H. **25**, 299 (2015).
[8] F. Mabood, W. A. Khan, and A. I. Ismail, Heat Transf. Asian Res. **44**, 293 (2005).
[9] J. A. Khan, M. Mustafa, T. Hayat, and A. Alsaedi, Can. J. Phys. **93**, 131 (2015).
[10] A. Majeed, A. Zeeshan, N. Amin, N. Ijaz, and T. Saeed, J. Therm. Anal. Calorim. **143**, 2545 (2021).
[11] S. W. Wong, M. A. O. Awang, A. Ishak, and I. Pop, J. Aerosp. Eng. **27**, 26 (2012).
[12] B. Gebhart, J. Fluid Mech. **14**, 225 (1962).
[13] K. Das, J. Mech. Sci. Technol. **28**, 1881 (2014).
[14] A. M. Megahed, Appl. Math. Mech. **36**, 1273 (2015).
[15] A. S. Gupta, Acta Mech. **22**, 281 (1975).
[16] T. Hayat, Z. Abbas, and S. Asghar, Commun. Nonlinear Sci. Numer. Simul. **13**, 2177 (2008).
[17] A. M. Saleem, and M. A. E. Aziz, Appl. Math. Model. **32**, 1236 (2008).
[18] M. A. E. Aziz, and T. Nabil, Math. Probl. Eng. **2012**, 454023 (2012).
[19] D. Pal, Comput. Math. Appl. **66**, 1161 (2013).
[20] A. Majeed, A. Zeeshan, S. Ali, and F. M. Noori, Trans. A. Razmadze Math. Inst. **76**, 57 (2022).
[21] A. Majeed, A. Zeeshan, N. Amin, N. Ijaz, and T. Saeed, J. Therm. Anal. Calorim. **143**, 2545 (2021).
[22] L. Zhang, M. M. Bhatti, M. Marin, and S. Mekheimer, Entropy. **22**, 1070 (2020).
[23] M. Marin, M. I. A. Othman, A. R. Seadawy, and C. Carstea, J. Taibah Univ. Sci. **14**, 653 (2021).
[24] A. Majeed, N. Amin, A. Zeeshan, R. Ellahi, S. M. Sait, and K. Vafai, Int. J. Numer.Methods Heat Fluid Flow. **30**, 4955 (2020).
[25] M. G. Reddy, Ain Shams Eng. J. **5**, 169 (2014).